


RESEARCH ARTICLE

Chronic low-level JUUL aerosol exposure causes pulmonary immunologic, transcriptomic, and proteomic changes

Terek Been^{1,2} | Bayan Alakhtar³ | Hussein Traboulsi² | Thupten Tsering^{2,4} | Alexandra Bartolomucci^{2,4} | Nicole Heimbach^{1,2} | Sofia Paoli^{1,2} | Julia Burnier^{2,4} | Koren K. Mann^{1,5} | David H. Eidelman^{2,6} | Carolyn J. Baglole^{1,2,3,4,6} 

¹Department of Pharmacology & Therapeutics, McGill University, Montreal, Quebec, Canada

²Research Institute of the McGill University Health Centre, Montreal, Quebec, Canada

³Division of Experimental Medicine, McGill University, Montreal, Quebec, Canada

⁴Department of Pathology, McGill University, Montreal, Quebec, Canada

⁵Department of Oncology, Lady Davis Institute for Medical Research, Jewish General Hospital, Montreal, Quebec, Canada

⁶Department of Medicine, McGill University, Montreal, Quebec, Canada

Correspondence

Carolyn J. Baglole, Department of Pharmacology & Therapeutics, McGill University, 1001 Decarie Blvd (EM22248), Montreal, QC H4A3J1, Canada.
 Email: carolyn.baglole@mcgill.ca

Funding information

FRQ | Fonds de Recherche du Québec - Santé (FRQS); Gouvernement du Canada | Canadian Institutes of Health Research

Abstract

E-cigarettes currently divide public opinion, with some considering them a useful tool for smoking cessation and while others are concerned with potentially adverse health consequences. However, it may take decades to fully understand the effects of e-cigarette use in humans given their relative newness on the market. This highlights the need for comprehensive preclinical studies investigating the effects of e-cigarette exposure on health outcomes. Here, we investigated the impact of chronic, low-level JUUL aerosol exposure on multiple lung outcomes. JUUL is a brand of e-cigarettes popular with youth and young adults. To replicate human exposures, 8- to 12-week-old male and female C57BL/6J mice were exposed to commercially available JUUL products (containing 59 mg/ml nicotine). Mice were exposed to room air, PG/VG, or JUUL daily for 4 weeks. After the exposure period, inflammatory markers were assessed via qRT-PCR, multiplex cytokine assays, and differential cell count. Proteomic and transcriptomic analyses were also performed on samples isolated from the lavage of the lungs; this included unbiased analysis of proteins contained within extracellular vesicles (EVs). Mice exposed to JUUL aerosols for 4 weeks had significantly increased neutrophil and lymphocyte populations in the BAL and some changes in cytokine mRNA expression. However, BAL cytokines did not change. Proteomic and transcriptomic analysis revealed significant changes in numerous biological pathways including neutrophil degranulation, PPAR signaling, and xenobiotic metabolism. Thus, e-cigarettes are not inert and can cause significant cellular and molecular changes in the lungs.

Abbreviations: Acsbg1, acetyl-CoA synthetase; ALB, albumin; Apoa2, apolipoprotein A2; Acox2, acetyl-CoA oxidase-2; BAL, bronchoalveolar lavage; Bpifb1, BPI fold-containing family B member; Clca1, calcium-activated chloride channel regulator 1; Cox-2, cyclooxygenase-2; Cpt1, carnitine palmitoyltransferase; Cyp2W1, cytochrome P4502W1; DPBS, Dulbecco's PBS; EtOH, ethanol; EV, extracellular vesicle; EVALI, vaping-associated lung injury; Fabp7, fatty acid binding protein; Fads2, fatty acid desaturase 2; Ift140, intraflagellar transport protein 140; iNOS, inducible nitric oxide synthase; Lcn2, lipocalin 2; MMP, matrix metalloproteinase; MPO, myeloperoxidase; NE, neutrophil elastase; NET, neutrophil extracellular trap; NHBE, normal human bronchial epithelial cells; NTA, nanoparticle tracking analysis; PFA, paraformaldehyde; PG, propylene glycol; Pigr, polymeric immunoglobulin receptor; Plin1, perilipin; PPAR, peroxisome proliferator-activated receptor; Rpia, ribose-5-phosphate isomerase; Scd4, stearoyl-CoA desaturase 4; Scgb3a1, secretoglobin family 3A; Slc27, SLC27 family of fatty acid transport protein; STRING, search tool for retrieval of interacting genes; TEM, transmission electron microscopy; Tg, thyroglobulin; THC, tetrahydrocannabinol; Tnfsf4, tumor necrosis factor ligand superfamily member 4/OX40L; VEA, vitamin E acetate; VG, vegetable glycerin.

This is an open access article under the terms of the [Creative Commons Attribution-NonCommercial-NoDerivs](https://creativecommons.org/licenses/by-nc-nd/4.0/) License, which permits use and distribution in any medium, provided the original work is properly cited, the use is non-commercial and no modifications or adaptations are made.

© 2023 The Authors. *The FASEB Journal* published by Wiley Periodicals LLC on behalf of Federation of American Societies for Experimental Biology.

Health Research (IRSC), Grant/Award Number: HEV-17889, 168836 and 162273; Ministry of Education – Kingdom of Saudi Arabi (MOE); Quebec Respiratory Health Network

KEYWORDS

e-cigarette, extracellular vesicles, inflammation, pulmonary system, RNA-sequencing

1 | INTRODUCTION

Tobacco use is a major global risk factor for disability and premature loss of life.¹ Because of the known health risks, many adult smokers report wanting to quit, but less than ten percent succeed in quitting annually.² E-cigarettes were developed in the early 2000s as a smoking cessation tool designed to simulate the act of smoking by delivering nicotine to the brain with the hope of exposing individuals to fewer toxic chemicals compared to traditional tobacco cigarettes.³ E-cigarettes typically consist of a battery, a vaporizer which consists of the vaporization chamber and a heating unit called the atomizer, and a liquid cartridge that holds the e-liquid.⁴ E-liquids contain varying amounts of humectants, most often a mix of propylene glycol (PG) and vegetable glycerin (VG), flavorings, and nicotine.⁵ There are thousands of different flavors available on the market.⁶ Although many ingredients in e-liquids are ‘Generally Recognized as Safe’ for oral consumption, there is little data on their safety when aerosolized and subsequently inhaled.⁷ Moreover, each device has a heating coil with varying metal contents, and these metals can be found in both the liquid and aerosol.^{8–11}

While e-cigarettes may aid in smoking cessation, their use has increased among non-smokers. E-cigarettes are particularly popular among youth, with 19.6% of high school students reporting current e-cigarette use in 2020.^{12,13} Notably, the pervasiveness of e-cigarette use among high school students significantly increased in 2015,¹⁴ coinciding with the development of JUUL, a brand of e-cigarettes whose device has a sleek design and came in an array of appetizing flavors. JUUL rapidly ascended in popularity,¹⁵ representing nearly three quarters of the dollar share of the US e-cigarette market in 2018, and remains one of the most popular e-cigarette brands among youth and young adults today³; most JUUL users use the product regularly.¹⁶ JUUL is a puff-activated, pod-style e-cigarette that is able to deliver a high nicotine content. It is estimated that a JUUL pod has the approximate nicotine content of one pack of cigarettes.¹⁷ To deliver higher nicotine, JUUL e-liquids contain a nicotine base and a weak organic acid (e.g., benzoic acid) that forms a nicotine salt once the device is activated.¹⁸ Nicotine salts are more tolerable when inhaled, allowing higher concentrations of nicotine to be used.¹⁹ Aside from nicotine, JUUL products are also available in several appealing flavors. The chemical flavorings can reach a cumulative concentration of over 10 mg/ml, with substantial variation in chemical constituents between flavored e-liquids.²⁰ Furthermore, JUUL uses a nichrome heating element and stainless steel

vapor path that can lead to leaching of metals such as chromium, iron, nickel, copper, and even lead into the emitted vapors.²¹ While there are limited health data regarding the significance of the presence of metals in e-cigarette aerosols, there is cause for concern with notable concentrations of toxic chemicals being inhaled by chronic users, where these metals may build up to toxic concentrations.²²

There is almost no information on the health impacts of inhaling aerosolized e-liquids containing nicotine salts (e.g., JUUL), and the current literature regarding acute and chronic health effects caused by e-cigarette use in general is largely inconclusive due to conflicting results.²³ However, there is emerging evidence that exposure to e-cigarette aerosols promotes pulmonary inflammation and oxidative stress,^{24–26} with some flavors inducing a more potent pro-inflammatory response.^{27,28} Some of the toxicity of e-cigarettes may be due to the humectants themselves which can induce airway irritation and cytotoxicity^{29–31}; chemicals produced from heating (e.g., aldehydes and acrolein) are also known to cause DNA damage and oxidative stress.³² However, comparison between experimental studies, and therefore the ability to draw conclusions is limited due in part to the lack of correlation with human puff topography (i.e., puff volume, puff interval, etc.) and objective measurements of exposure (e.g., cotinine).²³ There is also a scarcity of studies evaluating the broad-scale cellular and molecular changes caused e-cigarette exposure; this includes changes in the content of extracellular vesicles (EVs). EVs are membrane-bound vesicles that can modulate cellular expression and function. EVs contain cargo, including proteins and RNA, that when taken up by recipient cells can alter cellular function. EVs range in size from 30 to 1000 nm and can be categorized as exosomes, microvesicles, or apoptotic bodies. EVs are produced and released from cells under physiological conditions and in response to environmental exposures.^{33,34} EVs released in response to cigarette smoke for example can alter immune cell function,³⁵ and there is emerging evidence of EV release following e-cigarette use.³⁶ However, there is no information on EVs from JUUL use specifically although e-cigarette aerosol exposure increase platelet and endothelial-derived EVs.³⁷ Although JUUL was recently banned in the United States, many individuals have previous exposure to JUUL products and in other countries continue to use this brand of e-cigarettes. Thus, there is a need to assess the health impact of JUUL using exposure parameters that replicate human use patterns. Herein, we show that low-level chronic exposure to JUUL e-cigarette aerosols has local

immunomodulatory effects, and drastically changes protein and RNA expression in important pulmonary sites.

2 | METHODS

2.1 | Animals

C57BL/6J mice were purchased from the Jackson Laboratory and bred in-house. Male and female mice (age 8–12 weeks) were used for experiments. All procedures were approved by the McGill University Animal Care Committee and carried out in accordance with the Canadian Council on Animal Care.

2.2 | JUUL products

Commercially available, mango-flavored JUUL products containing 59 mg/ml nicotine were used. Mango-flavored pod cartridges were purchased from a local vape shop and were selected because fruit flavors are the most popular among e-cigarette users of various age demographics.³⁸ A standard commercial JUUL device was also used. The control liquid was composed of a 30:70 ratio of PG/VG purchased from Fusion Flavors (fusionflavors.ca).

2.3 | Animal exposures

Mice were randomly allocated to one of three groups: air, vehicle (PG/VG), or JUUL (mango). Exposures were performed using the SCIREQ® inExpose™ system equipped with an extension for JUUL. Exposure parameters and the puff profile were programmed using the flexiWare software. Mice were exposed to a puff regime consisting of three 20-min exposures per day for 4 weeks³⁹; this length of exposure in mice is roughly equivalent to 3 years in humans.⁴⁰ The puff regime was 1 puff per minute with a 78 ml puff volume, 2.4 s puff duration, with three hours between exposure sessions. These puff topography and usage parameters are consistent with human use patterns.^{29–31} Air-exposed mice were placed in the exposure apparatus for the equivalent length of time as the experimental groups. Mice were sacrificed the morning after the last exposure.

2.4 | Tissue harvest and BAL

Mice were anesthetized with 0.7 ml intraperitoneal injection of Avertin (2,2,2-tribromoethanol, 250 mg/kg i.p.; Sigma-Aldrich, St. Louis, MO) and euthanized by exsanguination via cardiac puncture. The lungs were excised and lavaged

with 0.5 ml of PBS. The BAL was centrifuged, and the supernatant was separated from cells. BAL cells were resuspended in PBS, counted, and 50 000 cells were then mounted onto slides using a CytoSpin (Thermo Scientific; Waltham, MA) and stained with Three Step Stain (Thermo Scientific, Waltham, MA). The remaining BAL cells were processed for RNA extraction. The right lung was filled with paraformaldehyde (PFA) and placed in PFA for fixation. The left lung tissue was frozen immediately in liquid nitrogen and stored at -80°C for subsequent protein and RNA analysis.

2.5 | qRT-PCR

Total RNA was extracted using a TRIzol Reagent and contaminating DNA was removed with an Aurum Total RNA Mini Kit (Bio-Rad) as per the manufacturer's instructions. The SYBR Green Master Mix (Bio-Rad) was used for the PCR using protocols previously described.³² All results were normalized using 18s rRNA as the housekeeping gene. Fold change was calculated using the $-\Delta\Delta\text{Ct}$ method, and results are presented as fold-change normalized to the housekeeping gene.³³ Sequences of primers used are in Table 1.

2.6 | Histology

The lungs were dissected rinsed with PBS, fixed in 4% PFA, embedded in paraffin and consecutive 4 μm sections of the lung were sectioned. Then, the slides were deparaffinized with xylene three times for 5 min each and hydrated with an ethanol gradient (100%–70%). Slides were dipped twice in 100% EtOH for 5 min each, one time in 95% EtOH and one time in 70% EtOH for 5 min each, and then washed with water for 5 min with MQ H₂O for 2 min. Antigen retrieval was performed using antigen retrieval solution (1X TRIS/EDTA pH9 and Tween-20). Slides were washed twice for 5 min each with wash buffer (TBS plus 0.025% Triton X-100) and then incubated in 4.5% H₂O₂ in 24 mM NaOH for 15 min, followed by rinsing three times with the wash buffer for 5 min each. Then, slides were blocked in 10% donkey/goat normal serum in wash buffer for 30 min. After, slides were incubated in Fc block plus mouse HRP (1:100) for 30 min followed by incubation with the primary antibody Ly6B (BioRad, Cat# MCA771GA) or CD8 (1:50) (eBioscience, Cat#14-0081-82) diluted in antibody buffer (1:1000 of donkey/goat normal serum in wash buffer) at room temperature for 30 min. Slides were then rinsed three times for 5 min each and incubated with the corresponding secondary antibody (1:2) (Goat pAp to Rat IgG+ HRP polymer) (Abcam, Cat#214882) diluted in antibody buffer for 30 min then washed four times with wash buffer 5 min each. Next, a short incubation of 4 min with DAB substrate

TABLE 1 Primer sequences for qRT-PCR

Target	Sequence
<i>tnfa</i>	5'-CCAAAGGGATGAGAAGTTCC-3' 3'-CTCCACTGGTGGTTTGCTA-3'
<i>il1β</i>	5'-AAGGAGAACCAAGCACGACAAAA-3' 5'-TGGGGAAGCTCTGCAGACTCAAAC-3'
<i>il6</i>	5'-TGATGCACTTGCAGAAAACAA-3' 5'-GGTCTTGGTCTTAGCCACTC-3'
<i>muc5B</i>	5'-TTACACCTGGCACACAATGG-3' 5'-TCCAGCTTCTGCAAGTTTCC-3'
<i>sod2</i>	5'-TTCTTTGGCTCATTGGGTCCTT-3' 5'-GATAAACAGGGGCTTCGCTGAT-3'
<i>nqo1</i>	5'-GCGGCTCCATGACTCTCTTCA-3' 5'-ACGGTTTCCAGACGTTTCTTCC-3'
<i>18s rRNA</i>	5'-GGACATCTAAGGGCATCACA-3' 5'-AGGAATTGACGGAAGGGCAC-3'
<i>il34</i>	5'-TACAGCCACCTCTGCTTGTG-3' 5'-GCAAGATACGGCATTGGTT-3'
<i>lcn2</i>	5'-CCC CAT CTC TGC TCA CTG TC-3' 5'-TTT TTC TGG ACC GCA TTG-3'
<i>col1a1</i>	5'-CAGACTGGCAACCTCAAGAA-3' 5'-CAGTGACGCTGTAGGTGAAG-3'
<i>mmp13</i>	5'-GCTTAGAGGTGACTGGCAAAC-3' 5'-TCTGGTCAAATTCAGTGGTGTC-3'
<i>adamts4</i>	5'-CAGTCACCTCTAAGCCAAAGAAA-3' 5'-CTTCCGGCGTAGGATGTGAG-3'
<i>plin1</i>	5'-TGAAGCAGGGCCACTCTC-3' 5'-GACACCACCTGCATGGCT-3'

was used to visualize staining, followed by 20s of hematoxylin to counterstain. Finally, slides were dehydrated by being dipped once in 95% EtOH for 2 min, twice in 100% EtOH for 60 s each, and three times in xylene 30 s each. Finally, slides were mounted using Permount mounting media. Staining was visualized using automated digital microscopy system (Zeiss AxioScan slide scanner) and analyzed (QuPath-0.2.3) by quantifying the percentage of positive stained cells over the total number of cells.

2.7 | EV enrichment and characterization

EVs were enriched using previously established protocols.^{41,42} In short, 300 μl of cell-free BAL fluid was enriched for EVs using ultracentrifugation. First, the BAL fluid was centrifuged at 300g for 10 min at 4°C to remove cell debris. The supernatant was collected and re-centrifuged at 2000g for 10 min at 4°C to pellet apoptotic bodies. The

remaining supernatant was transferred to 1 ml polycarbonate tubes (Beckman Coulter) and ultracentrifuged using TLA 120.2 in Beckman Coulter Optima MAX-XP at 100000g for 70 min at 4°C. The EV pellet obtained was washed with PBS and ultracentrifuged again at 100000g for 70 min at 4°C.⁴² EVs underwent nanoparticle tracking analysis (NTA) and were imaged using transmission electron microscopy (TEM). For NTA, 10 μl of EVs were diluted in 490 μl of PBS, run on a Nanosight NS500 system (Nanosight Ltd., Amesbury, UK), and the concentration and size distribution were analyzed using the NTA 1.3 software (Malvern Panalytical). For TEM, EVs were fixed with 2.5% glutaraldehyde fixation solution (250 ml EMS, 50 ml 25% glutaraldehyde, 250 ml water). TEM copper grids were kept on a drop (20 μl of fixed EVs) facing down and left to settle for 20 min. TEM grids were washed with Dulbecco's PBS (DPBS) and stained with 2% uranyl acetate for 3 min and air-dried overnight. EVs images were taken using FEI Tecnai™ G2 Spirit BioTwin 120 kV Cryo-TEM.

2.8 | Proteomic analysis

EVs were analyzed using LC-MS/MS. Here, each sample was loaded onto a single stacking gel band to remove lipids, detergents, and salts. The single gel band containing all proteins was reduced with DTT, alkylated with iodoacetic acid, and digested with trypsin. Two μg of extracted peptides were re-solubilized in 0.1% aqueous formic acid and loaded onto a Thermo Acclaim Pepmap (Thermo, 75 μM ID × 2 cm C18 3 μM beads) precolumn and then onto an Acclaim Pepmap Easyspray (Thermo, 75 μM × 15 cm with 2 μM C18 beads) analytical column separation using a Dionex Ultimate 3000 uHPLC at 250 nl/min with a gradient of 2%–35% organic (0.1% formic acid in acetonitrile) over 3 h. Peptides were analyzed using a Thermo Orbitrap Fusion mass spectrometer operating at 120 000 resolution (FWHM in MS1) with HCD sequencing (15 000 resolution) at top speed for all peptides with a charge of 2+ or greater. The raw data were converted into *.mgf format (Mascot generic format) for searching using the Mascot 2.6.2 search engine (Matrix Science) against mouse protein sequences (Uniprot 2021) The database search results were loaded onto Scaffold Q+ Scaffold_4.9.0 (Proteome Sciences) for statistical treatment and data visualization. To perform a protein–protein interaction network analysis, the Search Tool for Retrieval of Interacting Genes (STRING) (<https://string-db.org>) database was employed. Active interaction sources for constructing the network include text mining, experiments, databases, and co-expression. The species was limited to “Mus musculus” and a minimum required interaction score was set to 0.4.

2.9 | Multiplex analysis

BAL fluid was sent for multiplex analysis of inflammatory markers to Eve Technologies (www.evetech.com). BAL cytokines were assessed using the Mouse Cytokine/Chemokine 31-Plex Discovery Assay[®]. The cytokines/chemokines that were part of this assay included eotaxin, G-CSF, GM-CSF, IFN γ , IL-1 α , IL-1 β , IL-2, IL-3, IL-4, IL-5, IL-6, IL-7, IL-9, IL-10, IL-12p40, IL-12p70, IL-13, IL-15, IL-17A, IP-10, KC, LIF, LIX, MCP-1, M-CSF, MIG, MIP-1 α , MIP-1 β , MIP-2, RANTES, TNF α , and VEGF-A.

2.10 | RNA-seq

BAL cells from male and female mice were pooled from each exposure category (air: two male, two female; PG/VG: three male, three female; JUUL: three male, three female). RNA was isolated using TRIZol,⁴³ quantified using Qubit (Thermo Scientific) and quality assessed with the 2100 Bioanalyzer (Agilent Technologies). RNAseq analysis was performed at the Institute for Research in Immunology and Cancer (IRIC) in Montreal, QC. Transcriptome libraries were generated using QIaseq FastSelect ribodepletion selection (Qiagen), followed by KAPA RNA HyperPrep (Roche). Sequencing was performed on the Illumina NextSeq500, obtaining approximately 50M single-end 75bp reads per sample. Raw data were assessed for quality with FastQC 0.11.9 and reports were aggregated using MultiQC.⁴⁴ Since FastQC reports did not indicate sequence quality or adapter content problems, data were not trimmed. Next, STAR 2.7.8a was used to align data to the mm10 genome from UCSC with ENSEMBL (ensGene) annotations. Samtools 1.12 was used to discard reads that were not uniquely mapped and merge technical replicates. Alignment quality, RNA-seq metrics, and PCR duplication rates were assessed using Picard Tools 2.23.3 through the functions CollectAlignmentSummaryMetrics, CollectRnaSeqMetrics, and MarkDuplicates, respectively. Finally, gene expression was counted using featureCounts from the Subread 2.0.1 package, and differential expression was assessed using DESeq2.⁴⁵ This analysis led to the identification of approximately 25 000 transcripts. The total number of genes is listed in Table S1 for all comparison groups. All supplemental data can be found at DOI: [10.17632/frhg8rc5d.1](https://doi.org/10.17632/frhg8rc5d.1). Gene ontology was performed for differentially expressed ($p < .05$) using Metascape.⁴⁶ Changes in mRNA expression of select genes were verified by qRT-PCR using individual RNA from an additional subset of BAL cell RNA as described above.

2.11 | Statistical analysis

Statistical analysis was performed with GraphPad Prism v6.0 (GraphPad Software, San Diego). A one or two-way ANOVA was used to determine differences between groups of more than two followed by the assessment of individual differences by a Holm-Sidak or Dunn's post hoc test. Differences between groups of two was performed using a t -test. A p -value $< .05$ was considered significant. Significance of the proteomic data was evaluated using the Scaffold software.

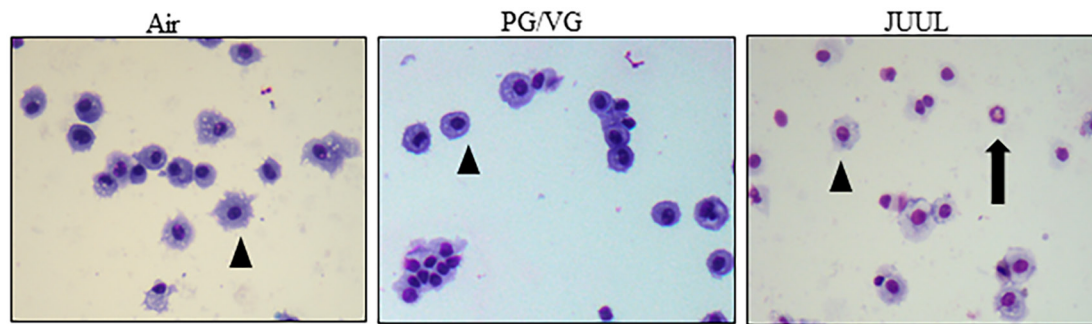
3 | RESULTS

3.1 | Low-level chronic JUUL aerosol exposure causes pulmonary inflammation

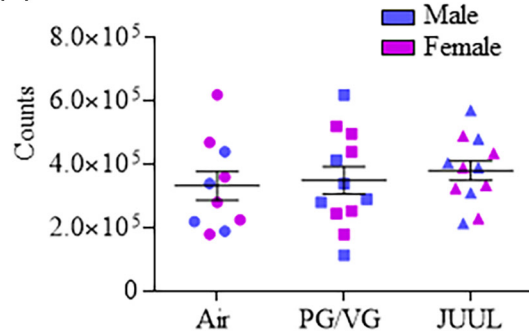
We previously published that an acute exposure to JUUL aerosols using an exposure regime that mimics a light or occasional user has minimal effect on lung inflammation.³⁹ However, there is concern that chronic use may lead to lung damage over time. Therefore, we now tested whether this same exposure scenario—but for a prolonged period of exposure (i.e., 4 weeks)—would cause an inflammatory response in the lungs and airways. Differential cell counts recovered from the BAL fluid (Figure 1A) revealed that although there were no significant differences in the number of total cells (Figure 1B) or macrophages (Figure 1C), there were significantly more lymphocytes (Figure 1D) and neutrophils (Figure 1E) in the JUUL group compared to the air control. The percentage of lymphocytes (Figure 1F) and neutrophils (Figure 1G) was also increased with JUUL exposure. There was no change in neutrophils or lymphocytes in the lung tissue (Figure 2). These data indicate that a low, but more chronic exposure regime to JUUL aerosols increases the presence of inflammatory cells in the airways.

We also assessed for the expression of pro-inflammatory and antioxidant genes in the whole lung homogenate by qRT-PCR (Figure 3). The pro-inflammatory genes assessed included *tnfa* (Figure 3A), *il1 β* (Figure 3B), and *il6* (Figure 3C). Only the mRNA expression of *il6* was significantly increased in response to JUUL (Figure 3C). Also assessed were the mRNA levels of *Muc5ac* (Figure 3D) and *Muc5b* (Figure 3E), genes which encode major mucus-producing proteins in the airways. Although there was a trend toward increased expression of *Muc5ac* and *Muc5b* in response to JUUL, this did not reach statistical significance. There was, however, a significant decrease in the expression of *Ace2* (Figure 3F), a key anti-inflammatory component of the renin-angiotensin system and the receptor for the SARS-Cov-2 virus responsible for the

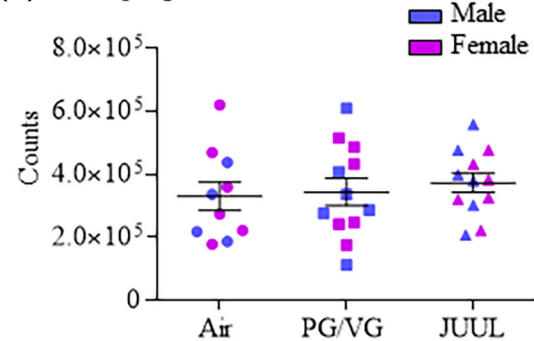
(A) BAL Cells



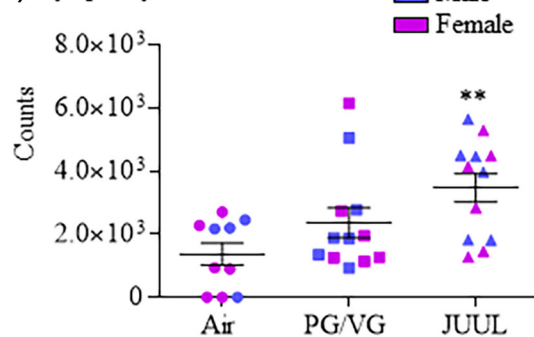
(B) Total Cells



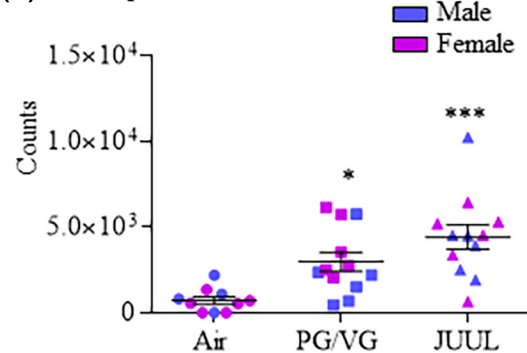
(C) Macrophages



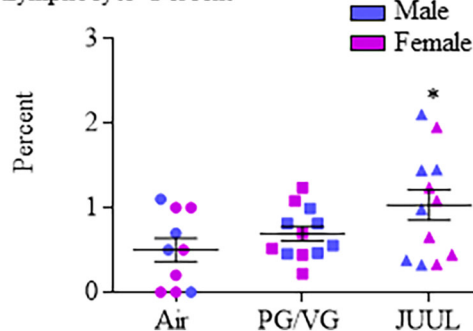
(D) Lymphocytes



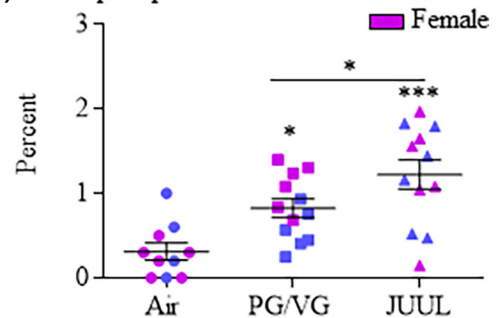
(E) Neutrophils



(F) Lymphocyte Percent



(G) Neutrophil percent



current COVID-19 pandemic, in response to both PG/VG and JUUL aerosols. *Ptgs2* mRNA, which encodes cyclooxygenase-2 (Cox-2) protein, was not altered by the exposure regime (Figure 3G). Finally, the expression of *Nqo1* (Figure 3H) and *Sod2* (Figure 3I), genes that are part of the antioxidant response, were increased in response to PG/VG. These data indicate that there are differential

changes in mRNA in lung tissue caused by inhalation of e-cigarette aerosols.

Lastly, we performed multiplex analysis of 31 different cytokines and chemokines in the BAL fluid. The majority of those analyzed were below the limit of detection for the assay (GM-CSF, IFN γ , IL-1 α , IL-1 β , IL-3, IL-4, IL-5, IL-6, IL-7, IL-9, IL-10, IL-12 (p40), IL-12 (p70), IL-13,

FIGURE 1 Chronic exposure to e-cigarette aerosols increases pulmonary inflammation. (A) BAL cells—Representative images of BAL cells with the major cell type being macrophages (arrowheads). Note the presence of neutrophils in BAL of the JUUL-exposed mice (arrow). (B) Total cells—there was no significant difference in the number of total cells in the BAL. (C) Macrophages—there was no significant change in the total number of macrophages in the BAL. (D) Lymphocytes—There was a significant increase in the number of lymphocytes in the JUUL-exposed mice (** $p < .01$) compared to mice that received only room air. (E) Neutrophils—There was also a significant increase in the number of neutrophils in both the PG/VG ($p < .05$) and JUUL-exposed mice (** $p < .001$) compared to mice that received only room air for 4 weeks. (F) Lymphocyte percent—there was a significant increase in the percentage of lymphocytes only in the JUUL-exposed mice ($p < .05$). (G) Neutrophil percent—there was a significant increase in the percentage of neutrophils in both the PG/VG ($p < .05$) and JUUL-exposed mice (** $p < .001$); the percentage of neutrophils was also significantly higher in the BAL of JUUL-exposed mice compared to those exposed to aerosolized PG/VG ($p < .05$). Results are expressed as the means \pm SEM ($n = 10$ – 12 mice per group and are the compilation of two independent experiments).

IL-17A, KC, LIF, LIX, MCP-1, M-CSF, MIP-1 α , MIP-1 β , RANTES, and TNF- α). For the cytokines that were detectable, such as eotaxin (Figure 4A), G-CSF (Figure 4B), IL-2 (Figure 4C), IL-15 (Figure 4D), IP-10 (Figure 4E), MIG (Figure 4F), MIP-2 (Figure 4G), and VEGF (Figure 4H), there was no significant change in their levels upon PG/VG or JUUL exposures.

3.2 | Chronic, low-level JUUL aerosol exposure causes transcriptomic changes in airway cells

RNAseq analysis was performed to evaluate the extent to which JUUL aerosol exposure affected the transcriptional response of cells in the airway lumen, the majority of which are macrophages. Overall, these data revealed that there are dramatic changes in response to e-cigarette aerosols. The largest number of differentially expressed protein-coding genes (\geq twofold change) were uniquely upregulated by JUUL compared to PG/VG (1140), and 1043 of these were common when JUUL was compared to both Air and PG/VG (Figure 5A). In addition, 27 genes were common between the three comparison groups (PG/VG-Air, JUUL-Air, and JUUL-PG/VG) (Figure 5A); these genes included *Tnfsf4* (tumor necrosis factor ligand superfamily member 4/OX40L), which is present in macrophages and plays a role in inflammation⁴⁷; and *Cyp2w1* (cytochrome P4502W1), an orphan CYP that may play a role in phospholipid metabolism.⁴⁸ There were also a number of genes (303) that were upregulated by PG/VG alone. Enrichment analysis revealed that several genes upregulated by PG/VG are involved in superoxide metabolic processes including *Edn1*, *Nos2*, *Nox4*, *Nox1*, *Imm2l*, and *Duox1*. KEGG pathway analysis revealed significant differences between the comparison groups, with JUUL-PG/VG eliciting changes in pathways related to nitrogen metabolism, ECM-receptor interaction, nicotine addiction, PPAR signaling, and drug metabolism—cytochrome P450 (Figure 5B). GO biological processes were enriched for negative chemotaxis, secretion, and regulation of response to wounding (Figure 5C). Other

enriched pathways included those involved in the regulation of leukocyte chemotaxis and migration and included genes such as *Ccl1*, *Ccl2*, *Ccl5*, *Il33*, *Cx3cr1*, and *Cxcl17*; this is consistent with changes in immune cell populations (Figure 1). Complete Metascape analysis results are in Tables S2 and S3.

We performed similar analysis for genes whose expression was down-regulated (\geq twofold). Here, the largest change in differentially expressed genes occurred in response to PG/VG (Figure 5D; PG/VG vs. Air). KEGG pathway analysis revealed that JUUL reduced enrichment for Th1 and Th2 cell differentiation and ECM-receptor interaction (Figure 5E) and for GO Biological processes was regulation of cellular response to growth factor stimulus (Figure 5F). Complete Metascape analysis results for down-regulated genes are in Tables S4 and S5. We then selected key genes found within the pathway enrichment analysis for up- and down-regulated genes for verification by qRT-PCR. These genes were selected based on their presence in multiple pathways, diversity in function and differential fold-change. Thus, these genes reflect the multitude of genes expression that is increased/decreased by JUUL and/or PG/VG. This included *il34* (Figure 6A), *Col1a1* (Figure 6B), *Lcn2* (Figure 6C), *mmp13* (Figure 6D), *Adams-4* (Figure 6E), and *Plin1* (Figure 6F). Changes observed by qRT-PCR were similar to the RNAseq analysis.

3.3 | E-cigarette aerosols causes significant sex-specific changes to the pulmonary proteome

Next, we performed unbiased proteomic analysis of the cell-free BAL that underwent further enrichment for EVs. EVs are membrane-derived particles that contain cellular cargo, including proteins,⁴⁹ may play a role in cell–cell communication and serve as biomarkers for environmental exposures. However, there are currently no analyses of EVs in response to JUUL. Therefore, we performed unbiased LC–MS/MS analysis on EVs isolated from male and female mice, with comparison made to air controls as well as aerosolized PG/VG. EV size and concentration,

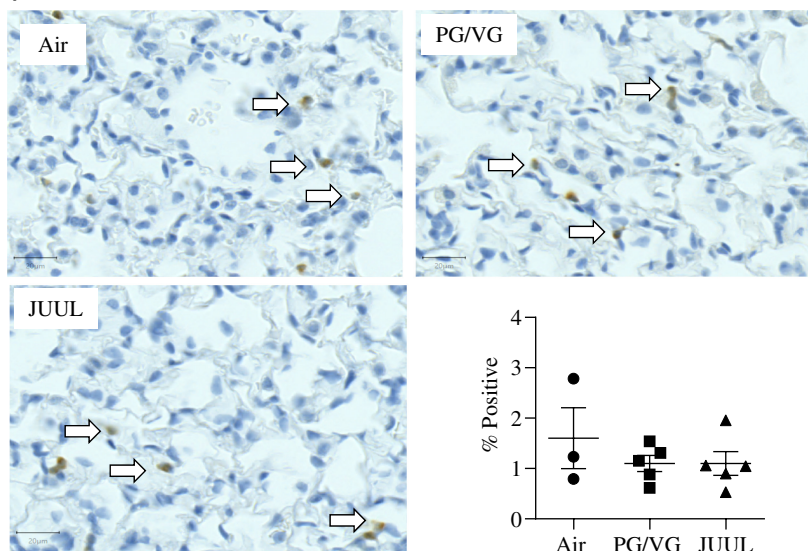
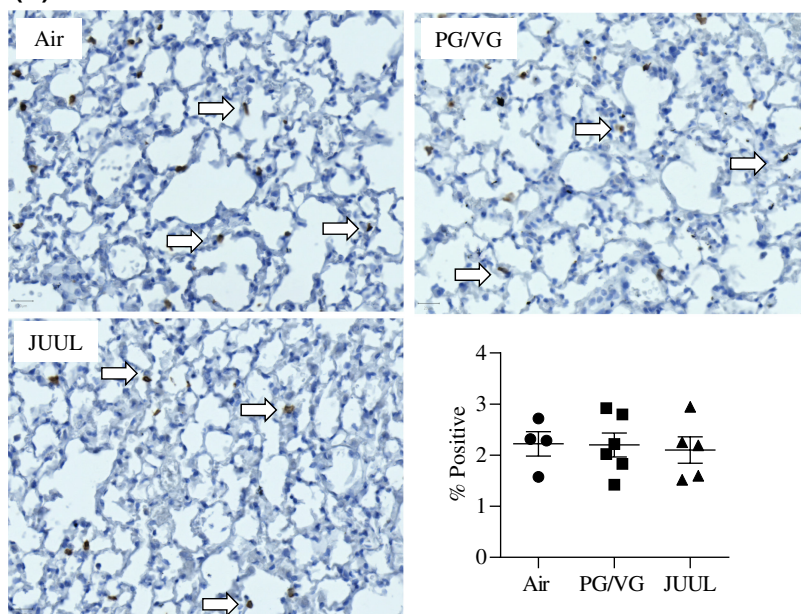
(A) Ly6B staining**(B)** CD8

FIGURE 2 E-cigarette aerosol exposure does not increase the presence of lymphocytes or neutrophils in the lung tissue. (A) Ly6B staining—There was no significant difference in the number of neutrophils (arrows) in the lung tissue in response to e-cigarette aerosol exposure for 4 weeks. (B) CD8—There was also no change in the number of CD8⁺ cells in the lung tissue (arrows). Results are expressed as the means \pm SEM ($n = 3$ –6 mice per group).

as measured using nanoparticle tracking analysis (NTA), showed a highly heterogeneous population of EV particles with broad size variation (100–1000 nm) (Figure 7A). There was no significant change in the number or size of EVs with either PG/VG or JUUL exposure (data not shown). EV morphology was also analyzed using TEM (Figure 7B), which showed EVs in a cup-shaped structure with heterogeneous particles.

A total of 1764 proteins were detected by LC–MS/MS. Quantitative profiling revealed that the majority of proteins (more than 1600) were present in all samples regardless of exposure (Figure 8A). Pathway analysis showed that these common proteins were not different between male and female mice and are involved in processes such as response to oxidative stress and regulation of vesicle-mediated

transport (Figure 8B; Table S6). However, there were significant differences in EV-enriched proteins in response to mango-flavored JUUL aerosols, although female mice had fewer proteins than males (Figure 8A). Proteins that were significantly changed in response to JUUL in female mice compared to air-exposed mice (Figure 8C) were intraflagellar transport protein 140 (Ift140), thyroglobulin (Tg), polymeric immunoglobulin receptor (Pigr), albumin (ALB), ribose-5-phosphate isomerase (Rpia), BPI fold-containing family B member 1 (Bpifb1), secretoglobin family 3A (Scgb3a1), and calcium-activated chloride channel regulator 1 (Clca1). There were more proteins detected in male mice exposed to JUUL (Figure 8C), including a cluster of cytochrome P450 enzymes (Cyp4a12b, Cyp2b9, Cyp2b10, Cyp2a5, Cyp2f2, and Cyp4b1).

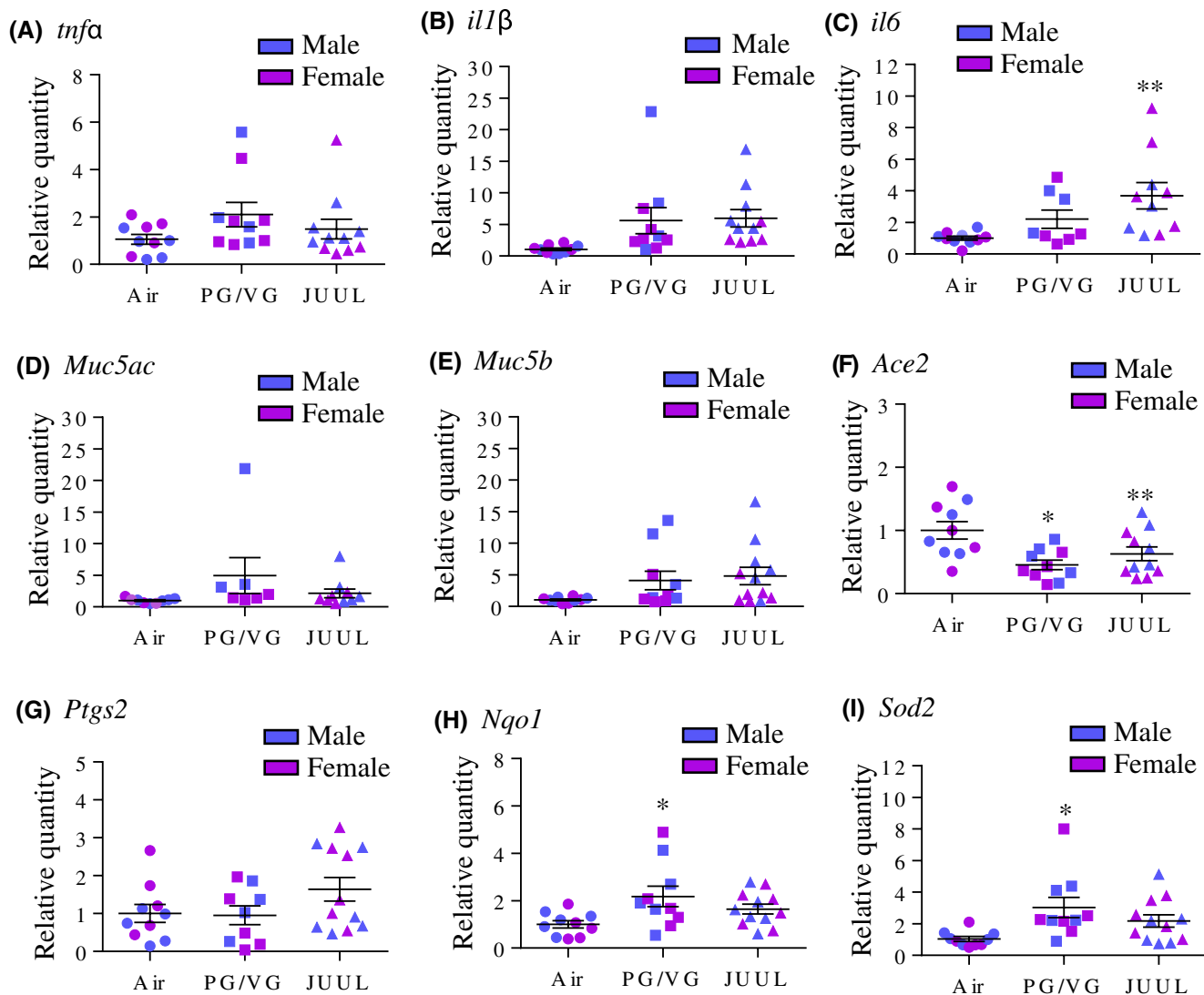


FIGURE 3 Changes in gene expression in response to e-cigarette aerosol exposure. There was no significant change in the mRNA expression for *tnfa* (A) or *il1b* (B) but there was a significant increase in *il6* expression (C) in response to JUUL exposure (** $p < .01$). There was also no change in *Muc5ac* (D) or *Muc5b* (E). There was a significant decrease in the expression of *Ace2* (F) in response to both PG/VG (* $p < .05$) and JUUL aerosol (** $p < .01$). There was no change in *Ptg2* mRNA expression (G). There was a significant increase in the expression of the antioxidant genes *Nqo1* (H) and *Sod2* (I) only in the PG/VG-exposed mice (* $p < .05$). Results are expressed as the means \pm SEM ($n = 10$ – 12 mice per group) and are the compilation of two independent experiments.

To then predict functional interactions between proteins detected in response to JUUL, we employed the STRING database. In female mice, the proteins were poorly connected (PPI enrichment p -value = .877) but there was functional enrichment for prenylation (Rab11b, Rab7, and Rac1; FDR = 0.0164) and GTP-binding (Rab11b, Rab7, Rac1, and Glud1; FDR = 0.0081) (Figure 9—inset). However, there were significant interactions among the proteins present in the JUUL-exposed male mice (PPI enrichment p -value $< 1.0 \times 10^{-16}$; Figure 9 and Table S7). Functional enrichment was observed for many biological and molecular pathways, including xenobiotic metabolic processes (Pon3, Cyp2f2, Cyp2a5, Ugt1a7c, Cyp2b2, Fmo2, Acsl1; FDR = 1.62×10^{-5} ; GO0006805), oxidation reduction processes (Cyp2f2, Por,

Cyp2a5, Aldh16a1, Mgst1, Cyb5r3, Fmo3, Dlat, Fmo2, Dlst, Cyp2b10, Acadm, Aldh3a2, Cyp4b1, Gpd1l, Cyb5a; FDR = 0.00011; GO:0055114), response to chemical (Pon1, Cyp2f2, Por, Cyp2a5, Mgst1, Ywhah, Canx, Psmc6, Ywhaz, Anxa5, Pon3, Acsl1, Apoc3, Serpina3k, Fmo2, Eprs, Ephx1, Ywhag, Ugt1a7c, Cyp2b10, Aldh3a2, Rpl27, Cyp4b1, Rtn4, Msn, Cyb5a, Iqgap1, Cul3; FDR = 0.0155; GO:0042221), chemical carcinogenesis (Mgst1, Ephx1, Ugt1a7c, Cyp2b10; FDR = 0.0123; mmu05204), fatty acid metabolism (Pon1, Pon3, Acsl1, Pccb, Acadm, Aldh3a2, Cyp4b1; FDR = 5.19×10^{-5} ; MMU-8978868) and neutrophil degranulation (Psmd2, Mgst1, Psmd3, Cyb5r3, Cand1, Psmd6, Vapa, Psmc2, Rab6a, Psmc3, Pgrmc1, Cap1, Rab7, Mvp, Iqgap1, H2-Q10; FDR = 2.02×10^{-9} ; MMU-6798695).

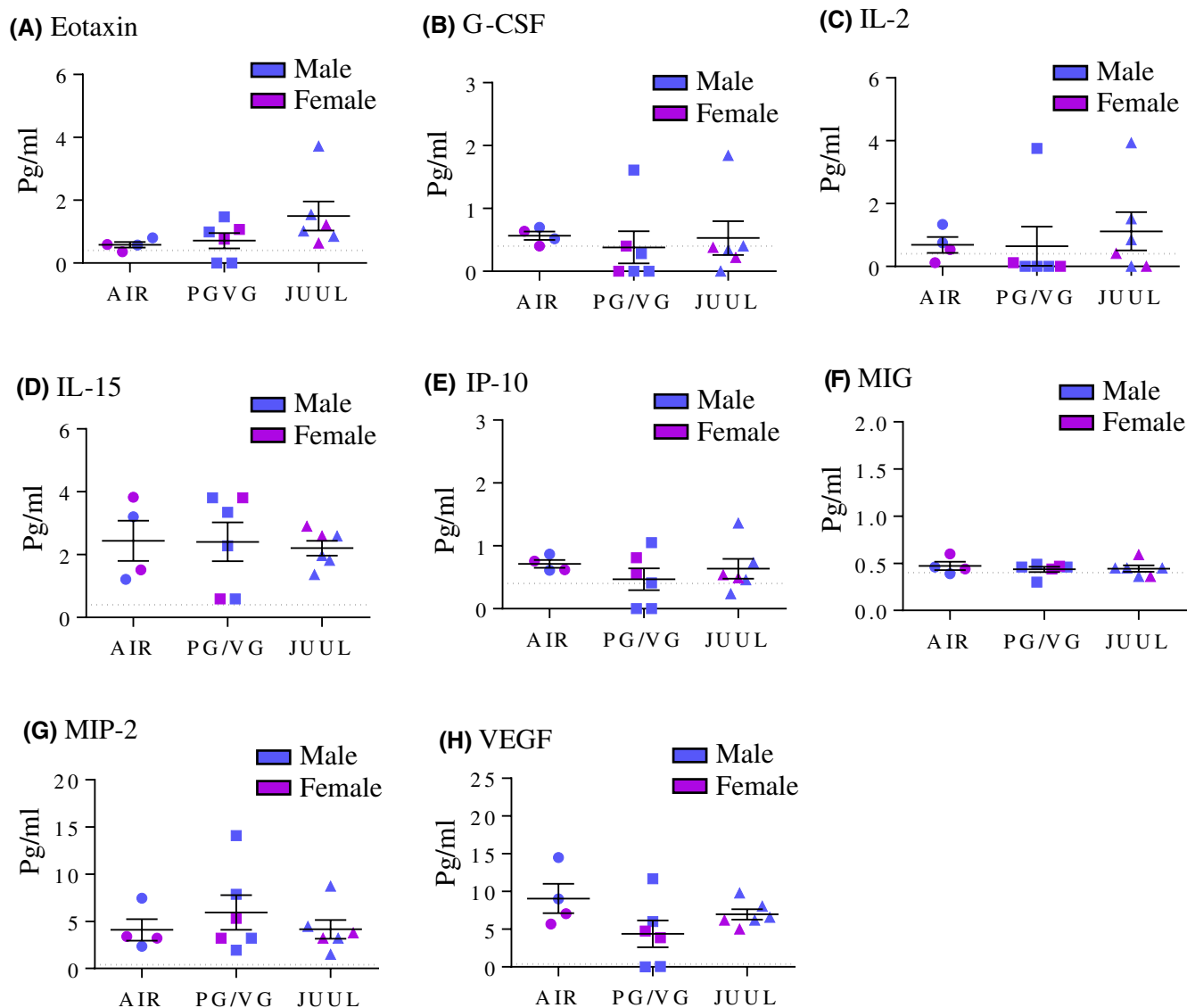
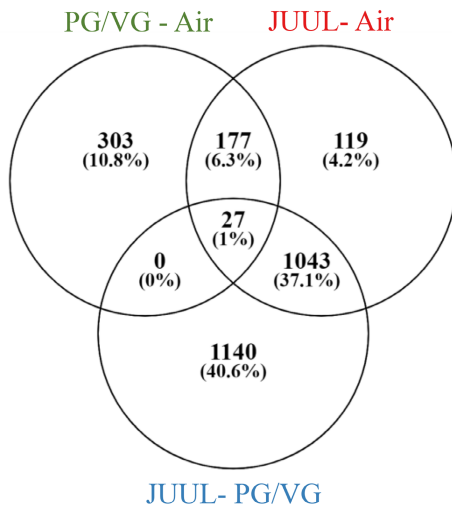
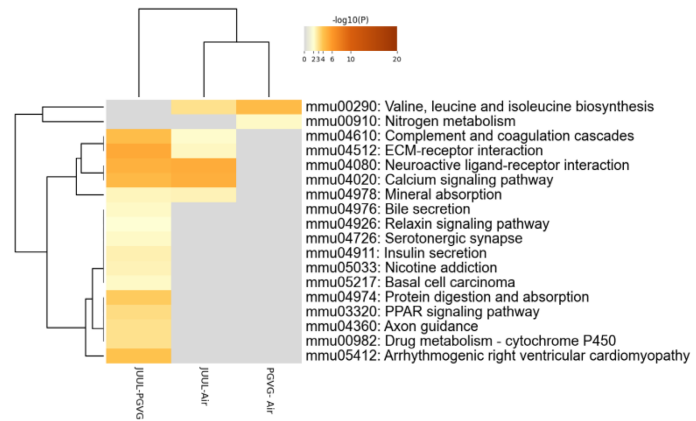
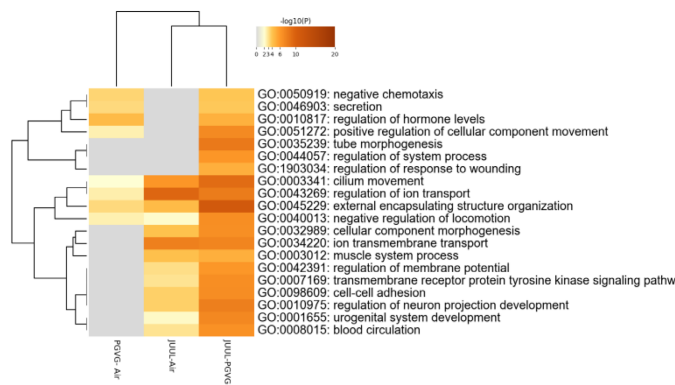
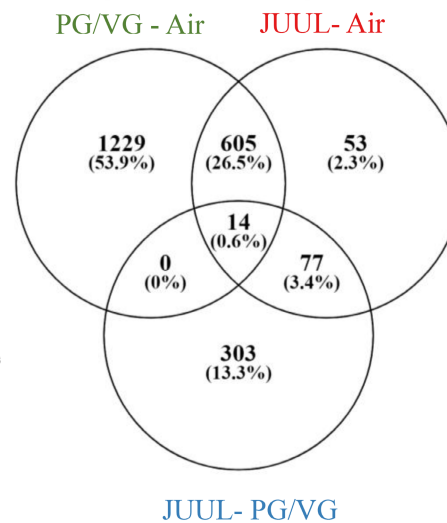
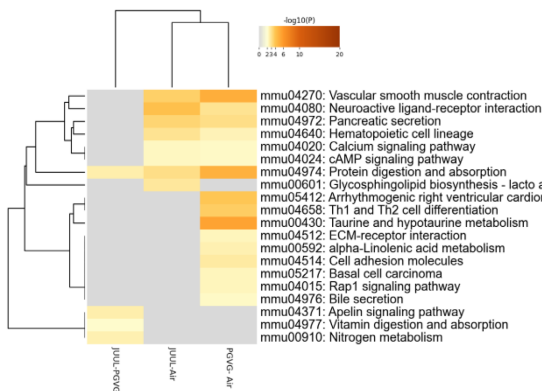
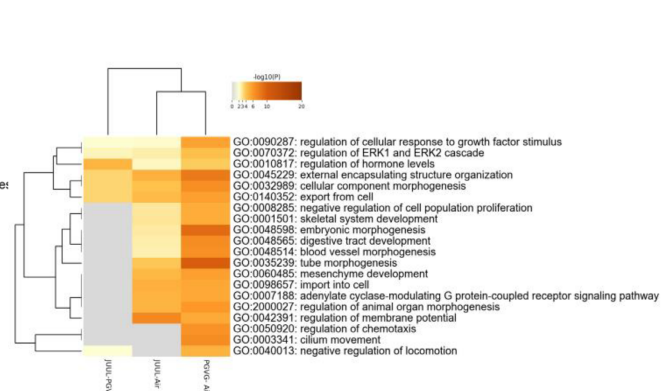


FIGURE 4 There is minimal change in the levels of BAL cytokines in response to e-cigarette aerosols. Cytokines that were detected in the BAL fluid included eotaxin (A), G-CSF (B), IL-2 (C), IL-15 (D), IP-10 (E), MIG (F), MIP-2 (G), and VEGF (H). Results are expressed as the means \pm SEM ($n = 4$ –6 mice per group).

To better understand sex-specific differences, we performed further analysis of proteins in the EV-enriched BAL between male versus female mice (t -test; $p < .05$);

these analyses revealed significant changes in the proteomic profile between female and male mice both in the absence of exposure (Figure 10A; air-only) and in

FIGURE 5 JUUL aerosol exposure for 4 weeks significantly changes gene expression in BAL cells. (A) Venn diagram—increased genes: exposure to JUUL aerosols for 4 weeks resulted in a unique transcriptional signature, with there being 1140 genes expressed by BAL cells compared to PG/VG; 1043 of these genes were common when compared to PG/VG and Air. Only 27 genes were expressed in BAL cells from all comparison groups. (B) KEGG Pathways analysis—increased genes: Heatmap shows the top-enriched KEGG pathways that were increased in response to JUUL aerosols. (C) GO Biological Processes—increased genes: Heatmap analysis shows the top-enriched pathways that were increased in response to JUUL. (D) Venn diagram—decreased genes: exposure to JUUL aerosols for 4 weeks resulted in a unique transcriptional signature, with there being 303 genes whose expression was decreased in BAL cells from JUUL-exposed mice compared to PG/VG; 77 genes were common when compared to both PG/VG and Air. Only 14 genes were expressed in BAL cells from all comparison groups. (E) KEGG Pathways analysis—decreased genes: Heatmap shows the top-enriched KEGG pathways that were decreased in response to JUUL aerosols. (F) GO Biological Processes—decreased genes: Heatmap analysis shows the top-enriched pathways that were decreased in BAL cells in response to JUUL compared to PG/VG-exposed mice.

(A) Venn diagram- increased genes**(B)** KEGG Pathway Analysis- increased genes**(C)** GO Biological Processes- increased genes**(D)** Venn diagram- decreased genes**(E)** KEGG Pathway Analysis- decreased genes**(F)** GO Biological Processes- decreased genes

response to JUUL aerosols (Figure 10B). Cyp4b1, Cyp2f2, and Cyp2b10 were still among the proteins that were significantly higher in JUUL-exposed male mice compared to JUUL-exposed female mice. Pathway enrichment analysis revealed that these proteins belong to top pathways associated with the phagosome (mmu04145),

neutrophil degranulation (R-MMU-6798695), ferroptosis (mmu04216), fatty acid metabolism (R-MMU-8978868), and COVID-19 (mmu05171) (Figure 10C; Table S8). Collectively these data highlight that JUUL exposure significantly alters proteins present in EV-enriched BAL fluid in a sex-dependent manner.

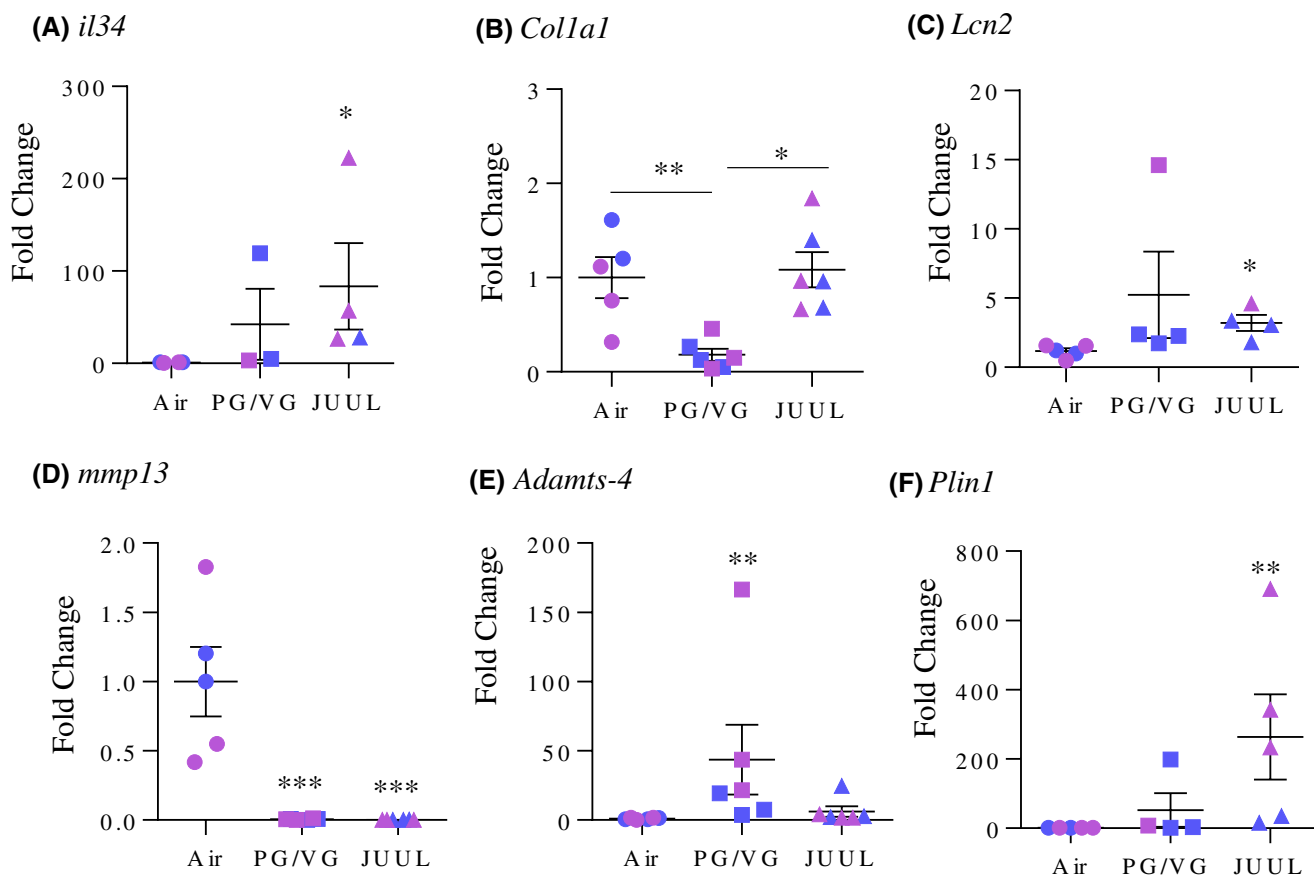


FIGURE 6 Validation of select genes in BAL cells. Genes selected for validation of the RNA-seq analysis included *il34* (A), *Col1a1* (B), *Lcn2* (C), *mmp13* (D), *Adamts-4* (E), and *Plin1* (F). Expression of these genes was significantly changed in BAL cells from JUUL-exposed mice (* $p < .05$; ** $p < .01$ compared to air-only mice). Results are expressed as the means \pm SEM ($n = 4$ –6 mice per group).

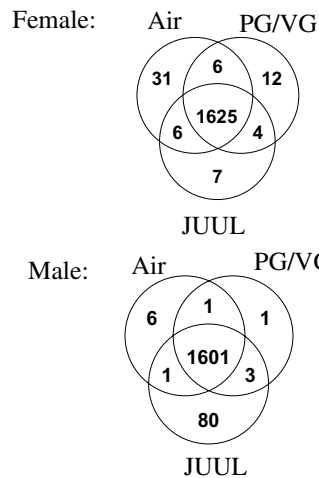
4 | DISCUSSION

There are concerns about the safety of e-cigarette use among never-smokers, and numerous studies suggest that these products may affect the lung and immune systems.^{50–52} However, results from these and other studies on e-cigarette toxicity are inconsistent, due to the vast array of e-liquid composition, brands, devices, and pre-clinical exposure protocols. Moreover, exceedingly few studies have utilized JUUL devices and e-liquids despite their popularity. To address this gap in knowledge, we recently published that an acute 3-day exposure regime which mimics light and moderate JUUL users increases pulmonary inflammation.³⁹ The current study not only adds to the growing evidence pertaining to the inflammatory outcomes caused by e-cigarette exposure but incorporates unbiased molecular investigation by utilizing proteomic and transcriptomic analysis. Our results demonstrate that prolonged inhalation of e-cigarette aerosols cause changes in pulmonary immune cell composition and alters gene and protein levels in the lungs.

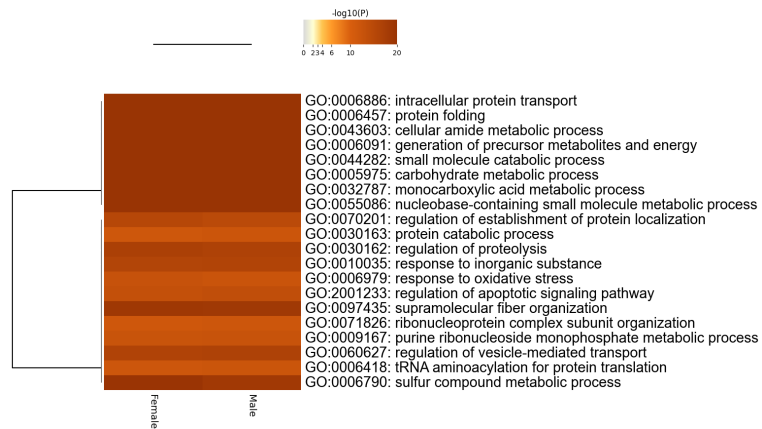
One of our most consistent observations is the presence of neutrophils in the lung lavage of mice that were

exposed to e-cigarette aerosols. Neutrophils, the most abundant circulating leukocytes, are a short-lived cell with a half-life in the circulation of approximately 1.5–12.5 h in mice.⁵³ Neutrophils are one of the first cell types recruited upon infection or insult and thus, are a hallmark of acute inflammation. Leukocytosis is the main respiratory immune alteration in traditional tobacco smokers^{54,55} but their recruitment to the lungs from e-cigarette exposures is variable.^{56,57} Our observation that neutrophils are increased in the BAL of both PG/VG and JUUL suggests that the neutrophilia observed is independent of nicotine or flavoring chemicals but may be the result of the solvent itself (PG/VG). These findings are in agreement with several other in vivo studies investigating the pulmonary outcomes of e-cigarette exposure, including the ability of inhaled aerosols to increase lung neutrophils.^{28,50,57} Moreover, as in this study using mango-flavored-JUUL products, the impact of different flavors is notable, particularly fruit flavors and tobacco flavors.^{57,58} However, not all studies show that e-cigarettes increase lung neutrophils,²⁵ and some studies show that PG/VG alone increases neutrophils in the lungs,⁵⁸ a finding that contrasts our results. These differences in outcomes may be

(A) Venn Diagrams



(B) Pathway Analysis



(C) Volcano Plots: Air Vs JUUL

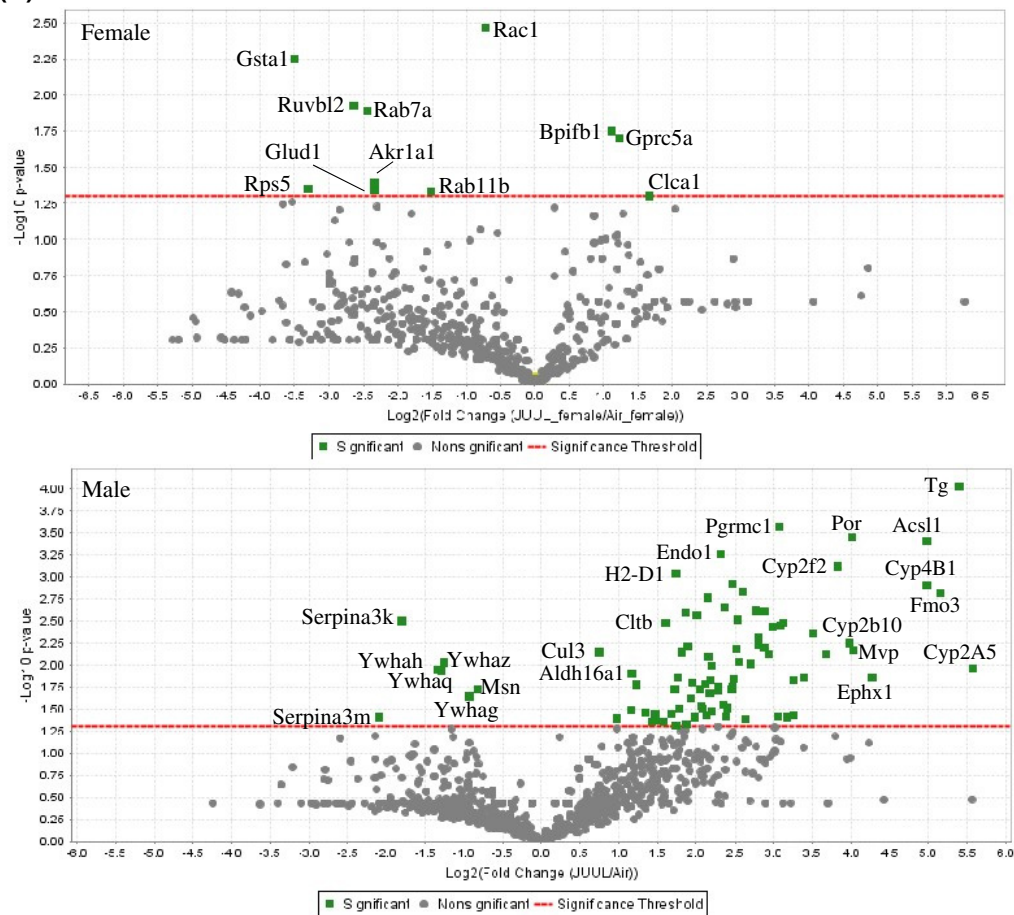
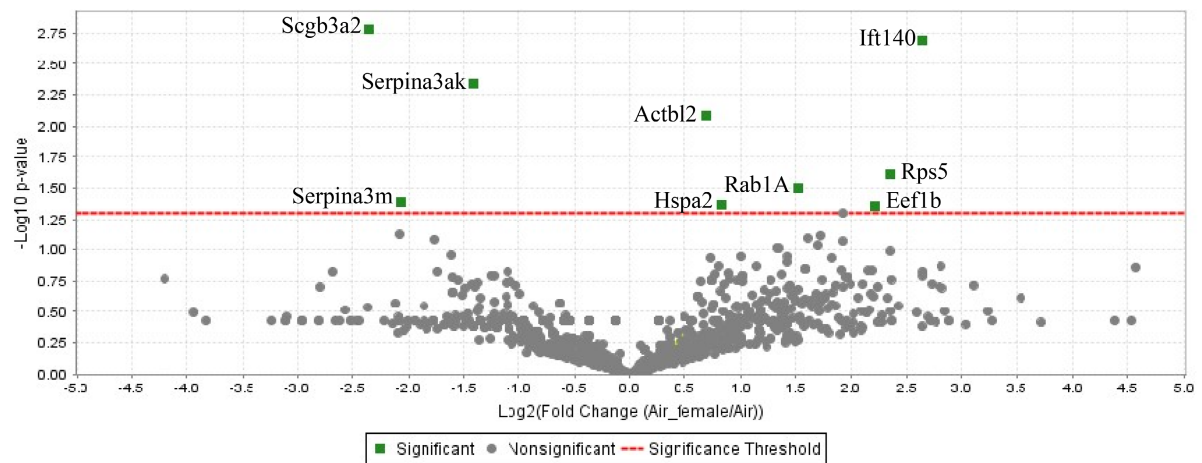


FIGURE 8 Proteomics analysis from EV-enriched BAL fluid reveals sex-specific differences in proteins. (A) Venn Diagrams—Note that the majority of proteins detected were common in all exposure group. In female mice, there were few proteins present only in this exposure group whereas in male mice there were more distinct proteins in EVs caused by JUUL exposure. (B) Pathway Analysis—Heatmap of pathways common in proteins found in EV-enriched BAL fluid. Analysis was performed in proteins detected in all three groups of exposed mice. (C) Volcano Plots: Air vs. JUUL—In female mice (top), the proteins significantly increased included *Ccl1*. There were more proteins significantly increased in male mice (bottom) and included numerous Cyp450 proteins (*t*-test; $p < .05$).

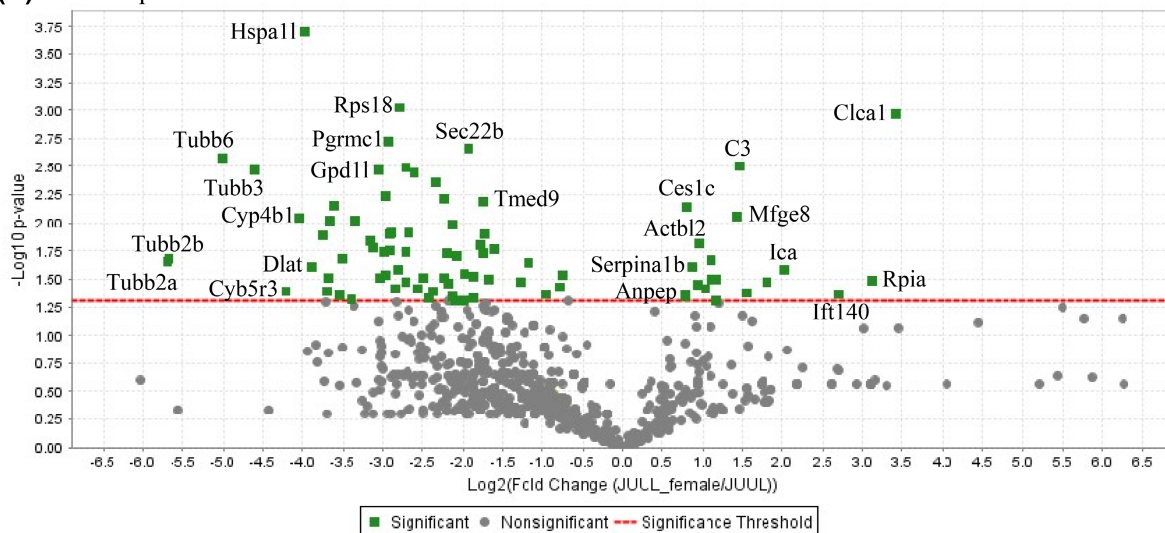
changes in morphology and function in response to e-cigarette aerosols, including phagocytosis and lipid metabolism.^{24,63,64} One of the limitations of this study is

that we did not perform functional analysis of the macrophages in response to pod-style e-cigarettes. This will be a focus of future experiments.

(A) Volcano plot- Air



(B) Volcano plot- JUUL



(C) Pathway Enrichment- JUUL

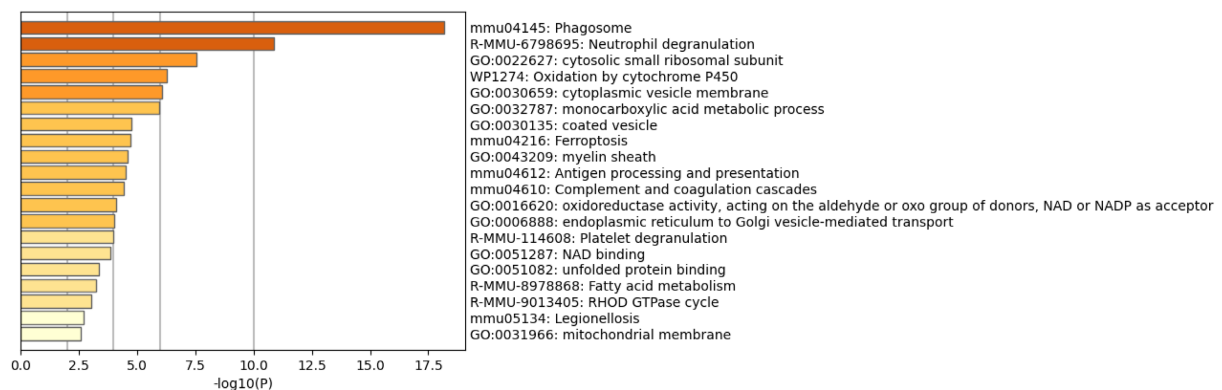


FIGURE 10 Comparison of proteins in EVs between male and female mice. (A) Volcano plot—Air: Proteins that were increased in male mice exposed only to room air compared to female mice were Ift140, Rps5, Hspa2, and Eef1b. (B) Volcano plot—JUUL—There were more proteins altered in JUUL-exposed male mice compared to female mice. (C) Pathway enrichment—JUUL—The pathways enriched in male JUUL-exposed mice include the phagosome, neutrophil degranulation, and oxidation by cytochrome p450.

(*Slc27a2*, *Slc27a5*), fatty acid desaturase 2 (*Fads2*), acetyl-CoA oxidase-2 (*Acox2*), acetyl-CoA synthetase (*Acsbg1*), perilipin (*Plin1*), stearoyl-CoA desaturase 4 (*Scd4*), and lipocalin 2 (*Lcn2*). The transcriptomic changes in genes associated with lipid metabolism are similar to changes in macrophages from smokers with and without COPD.⁶⁹ Moreover, both cigarette smoke and e-cigarette aerosols can cause cytoplasmic accumulation of lipids,^{24,70} indicative of altered lipid metabolism. Thus, these results support the notion that even a low-level exposure to JUUL may change lipid homeostasis within the lungs.

This altered transcriptional response to chronic low-level JUUL exposure, whereby there is enrichment in pathways associated with lipid metabolism, may have functional consequences related to an outbreak of respiratory illness termed vaping-associated lung injury (EVALI). EVALI was associated with adverse respiratory symptoms including shortness of breath, chest pain, cough, and hemoptysis²³ and in severe cases death. Since 2019, thousands of cases reported across the United States. EVALI has been strongly linked to e-cigarettes containing tetrahydrocannabinol (THC) where vitamin E acetate (VEA) was used as a diluent.⁷¹ An initial defining feature of EVALI was the presence of lipid-laden macrophages from the lungs,^{72,73} although the presence of foamy macrophages occurs in a variety of conditions and exposures including nicotine-containing e-cigarettes with PG/VG.²⁴ The changes seen in this study may have further implications for the development of acute lung injury in association with combined exposures, a scenario that is relevant for EVALI as many patients used both THC- and nicotine-based e-cigarette.⁷⁴ Moreover, symptoms of EVALI overlap with those of COVID-19.⁷⁵ Although there is controversy on whether e-cigarette use alters COVID-19 susceptibility or severity,⁷⁶ there is evidence that e-cigarette aerosol exposure augments the inflammatory response to other types of viral infection^{77,78} and in some cases may exacerbate symptoms of EVALI.⁷⁹ Thus, it is possible that prior e-cigarette use predisposes select individuals to adverse pulmonary outcomes associated with co-exposures due to subtle but significant molecular and cellular changes in the pulmonary microenvironment.

The transcriptomic changes were complemented with proteomic analysis of acellular EVs, which are linked to neutrophil chemotaxis⁸⁰ and could explain why there are more neutrophils in the lungs in response to JUUL in the absence of significant changes in key cytokines or chemokines. Our proteomic analysis of acellular BAL EVs highlights the dramatic difference in protein cargo caused by e-cigarette exposures. The most striking difference however was between male and female mice, a biological variable that is often overlooked in discovery-based studies. Here, JUUL-exposed male mice exhibited a greater

number of distinct proteins compared to female mice. Sex-dependent effects of e-cigarettes were also shown in a separate study, with e-cigarette-exposed male mice having increased pro-inflammatory cytokine release compared to female mice.⁸¹ In our study, pathway mapping comparing the protein profile of JUUL-exposed male versus female mice revealed enrichment in a number of pathways associated with immune function including neutrophil degranulation, phagosome, and platelet degranulation. Neutrophil degranulation may be of particular importance as the contents of neutrophil granules have been implicated in the pathophysiology of several lung disorders.⁸² The observation that there were more proteins associated with neutrophil degranulation in male mice may indicate higher release of contents and/or sequestration in EVs; similar changes in neutrophil activation have also been observed in a mouse model of JUUL exposure.⁸³ Furthermore, the dramatic differences in EV proteomics between male and female mice is a novel observation and highlight the importance of analysis of sex-specific differences at the molecular level. It is also noteworthy that there is enrichment of proteins important in ferroptosis, a necrotic type of programmed cell death caused by iron accumulation, lipid peroxidation, and oxidative stress; ferroptosis can be caused by smoke and is linked to the pathogenesis of smoke-related diseases such as COPD.⁸⁴

Another pathway in which there were notable sex-specific differences in acellular EV proteins was those related to xenobiotic metabolism, including the presence of a range of CYP450s (e.g., *Cyp2f2*, *Cyp2a5*, *Cyp4b1*, and *Cyp2b10*). EVs are known to contain CYP450s.⁸⁵ Metabolism of xenobiotics often leads to the production of highly reactive intermediates. These intermediates can directly interact with nearby proteins, fatty acids, and intracellular machinery resulting in overall dysfunction.⁸⁶ Metabolism of exogenous chemicals by cytochromes can also indirectly cause damage by inducing oxidative stress causing widespread damage to the cell. One of the CYPs that was significantly increased in EVs from JUUL-exposed male mice was *Cyp2f2*. *Cyp2f2* metabolizes naphthalene, a toxicant found in cigarette smoke and air pollution; naphthalene is also present in e-cigarette aerosols.⁸⁷ Female mice have less *Cyp2f2* and are also more susceptible to repeated naphthalene exposure.⁸⁸ Thus, our data is the first to show increased *Cyp2f2* in response to JUUL aerosol exposure, an increase where there was a sex-specific difference. Thus, this study provides novel information that sex-specific differences in pulmonary EV cargo not only informs on potential biological consequences of e-cigarette aerosol exposure but may also serve as biomarkers of e-cigarette use.

In summary, we have demonstrated that even low exposure to JUUL aerosols impact pulmonary outcomes

at the cellular and molecular levels. Both commercially available, mango-flavored JUUL products and the vehicle PG/VG significantly alter transcriptional regulation of important inflammatory genes and alter inflammatory cell populations in the airways. These changes were paralleled by observations of sex-specific differences in proteomic expression in acellular EVs. There are some inherent limitations of this study that may limit generalizability to humans, including the fact that mouse models do not fully recapitulate human physiology, including differences in lung cellularity, architecture, and physiology.^{39,89,90,91} In addition, exposures longer than 4 weeks to mimic more chronic use may give further insight into lung damage caused by JUUL exposure. Nonetheless, these findings highlight that these products are not inert and elicit significant pulmonary changes, supporting the need for further study into the effects of e-cigarette use.

AUTHOR CONTRIBUTIONS

Data curation and/or analysis: Terek Been, Hussein Traboulsi, Sofia Paoli, Bayan Alakhtar, Nicole Heimbach, Alexandra Bartolomucci, Thupten Tsering; Funding acquisition: Koren K. Mann, Carolyn J. Baglole; Investigation: Terek Been, Hussein Traboulsi, Carolyn J. Baglole; Methodology: Terek Been, Hussein Traboulsi, Sofia Paoli, Alexandra Bartolomucci., Julia Burnier, Thupten Tsering, Bayan Alakhtar; Koren K. Mann, Carolyn J. Baglole; Project administration: Koren K. Mann, Carolyn J. Baglole; Resources: Koren K. Mann, Carolyn J. Baglole; Supervision: Koren K. Mann, Carolyn J. Baglole; Intellectual contributions: Koren K. Mann, David H. Eidelman, Julia Burnier, Carolyn J. Baglole; Manuscript writing, review, and editing: Terek Been, Hussein Traboulsi, Sofia Paoli, Bayan Alakhtar, Julia Burnier, Thupten Tsering, Koren K. Mann, David H. Eidelman, Carolyn J. Baglole.

FUNDING INFORMATION

This work was supported by the Quebec Respiratory Health Research Network (QRHN) and the Canadian Institutes for Health Research (CIHR). C.J.B. is supported by a salary award from the Fonds de recherche du Québec-Santé (FRQ-S). H.T. was supported by fellowships from the Réseau de recherche en santé respiratoire du Québec (RSR) Scholarship and Meakins-Christie Laboratories. B.A. is supported by a Saudi Student Scholarship from the Ministry of Education (MOE).

DISCLOSURES

All authors certify that they have no affiliations with or involvement in any organization or entity with any financial interest or non-financial interest in the subject matter or materials discussed in this manuscript.

DATA AVAILABILITY STATEMENT

Supplemental tables containing proteomics and RNA-sequencing data in support of this study are available at Mendeley Data at doi: [10.17632/ftrhg8rc5d.1](https://doi.org/10.17632/ftrhg8rc5d.1). All remaining raw data are available from the corresponding author upon request.

ETHICS STATEMENT

All procedures involving mice were approved by the McGill University Animal Care Committee (Protocol number 2013-7421) and carried out in accordance with the Canadian Council on Animal Care Committee.

ORCID

Carolyn J. Baglole  <https://orcid.org/0000-0002-3107-0437>

REFERENCES

1. Lim SS, Vos T, Flaxman AD, et al. A comparative risk assessment of burden of disease and injury attributable to 67 risk factors and risk factor clusters in 21 regions, 1990–2010: a systematic analysis for the Global Burden of Disease Study 2010. *Lancet*. 2012;380:2224–2260.
2. Babb S, Malarcher A, Schauer G, Asman K, Jamal A. Quitting smoking among adults—United States, 2000–2015. *MMWR Morb Mortal Wkly Rep*. 2017;65:1457–1464.
3. Fadus MC, Smith TT, Squeglia LM. The rise of e-cigarettes, pod mod devices, and JUUL among youth: factors influencing use, health implications, and downstream effects. *Drug Alcohol Depend*. 2019;201:85–93.
4. Orellana-Barrios MA, Payne D, Mulkey Z, Nugent K. Electronic cigarettes—a narrative review for clinicians. *Am J Med*. 2015;128:674–681.
5. Thiri6n-Romero I, P6rez-Padilla R, Zabert G, Barrientos-Guti6rrez I. Respiratory impact of electronic cigarettes and “low-risk” tobacco. *Rev Invest Clin*. 2019;71:17–27.
6. Zhu SH, Sun JY, Bonnevie E, et al. Four hundred and sixty brands of e-cigarettes and counting: implications for product regulation. *Tob Control*. 2014;23 Suppl 3:iii3–iii9.
7. Kaur G, Muthumalage T, Rahman I. Mechanisms of toxicity and biomarkers of flavoring and flavor enhancing chemicals in emerging tobacco and non-tobacco products. *Toxicol Lett*. 2018;288:143–155.
8. Goniewicz ML, Knysak J, Gawron M, et al. Levels of selected carcinogens and toxicants in vapour from electronic cigarettes. *Tob Control*. 2014;23:133–139.
9. Williams M, Villarreal A, Bozhilov K, Lin S, Talbot P. Metal and silicate particles including nanoparticles are present in electronic cigarette cartomizer fluid and aerosol. *PLoS One*. 2013;8:e57987.
10. Olmedo P, Goessler W, Tanda S, et al. Metal concentrations in e-cigarette liquid and aerosol samples: the contribution of metallic coils. *Environ Health Perspect*. 2018;126:027010.
11. Hess CA, Olmedo P, Navas-Acien A, Goessler W, Cohen JE, Rule AM. E-cigarettes as a source of toxic and potentially carcinogenic metals. *Environ Res*. 2017;152:221–225.
12. Vallone DM, Cuccia AF, Briggs J, Xiao H, Schillo BA, Hair EC. Electronic cigarette and JUUL use among adolescents and young adults. *JAMA Pediatr*. 2020;174:277–286.

13. Wang TW, Neff LJ, Park-Lee E, Ren C, Cullen KA, King BA. E-cigarette use among middle and high school students—United States, 2020. *MMWR Morb Mortal Wkly Rep.* 2020;69:1310-1312.
14. Cullen KA, Ambrose BK, Gentzke AS, Apelberg BJ, Jamal A, King BA. Notes from the field: use of electronic cigarettes and any tobacco product among middle and high school students—United States, 2011–2018. *MMWR Morb Mortal Wkly Rep.* 2018;67:1276-1277.
15. Huang J, Duan Z, Kwok J, et al. Vaping versus JUULing: how the extraordinary growth and marketing of JUUL transformed the US retail e-cigarette market. *Tob Control.* 2019;28:146-151.
16. Willett JG, Bennett M, Hair EC, et al. Recognition, use and perceptions of JUUL among youth and young adults. *Tob Control.* 2019;28:115.
17. Goniewicz ML, Boykan R, Messina CR, Eliscu A, Tolentino J. High exposure to nicotine among adolescents who use Juul and other vape pod systems ('pods'). *Tob Control.* 2019;28:676-677.
18. Pankow JF, Kim K, McWhirter KJ, et al. Benzene formation in electronic cigarettes. *PLoS One.* 2017;12:e0173055.
19. Rao P, Liu J, Springer ML. JUUL and combusted cigarettes comparably impair endothelial function. *Tob Regul Sci.* 2020;6:30-37.
20. Omaye EE, McWhirter KJ, Luo W, Pankow JF, Talbot P. High-nicotine electronic cigarette products: toxicity of JUUL fluids and aerosols correlates strongly with nicotine and some flavor chemical concentrations. *Chem Res Toxicol.* 2019;32:1058-1069.
21. Pappas RS, Gray N, Halstead M, Valentin-Blasini L, Watson C. Toxic metal-containing particles in aerosols from pod-type electronic cigarettes. *J Anal Toxicol.* 2020;45:337-347.
22. Nemery B. Metal toxicity and the respiratory tract. *Eur Respir J.* 1990;3:202-219.
23. Traboulsi H, Cherian M, Abou Rjeili M, et al. Inhalation toxicology of vaping products and implications for pulmonary health. *Int J Mol Sci.* 2020;21:1-31.
24. Madison MC, Landers CT, Gu BH, et al. Electronic cigarettes disrupt lung lipid homeostasis and innate immunity independent of nicotine. *J Clin Invest.* 2019;129:4290-4304.
25. Garcia-Arcos I, Geraghty P, Baumlin N, et al. Chronic electronic cigarette exposure in mice induces features of COPD in a nicotine-dependent manner. *Thorax.* 2016;71:1119-1129.
26. Singh KP, Lawyer G, Muthumalage T, et al. Systemic biomarkers in electronic cigarette users: implications for noninvasive assessment of vaping-associated pulmonary injuries. *ERJ Open Res.* 2019;5:1-12.
27. Bengalli R, Ferri E, Labra M, Mantecca P. Lung toxicity of condensed aerosol from E-CIG liquids: influence of the flavor and the in vitro model used. *Int J Environ Res Public Health.* 2017;14:1-14.
28. Lerner CA, Sundar IK, Yao H, et al. Vapors produced by electronic cigarettes and e-juices with flavorings induce toxicity, oxidative stress, and inflammatory response in lung epithelial cells and in mouse lung. *PLoS One.* 2015;10:e0116732.
29. Behar RZ, Wang Y, Talbot P. Comparing the cytotoxicity of electronic cigarette fluids, aerosols and solvents. *Tob Control.* 2018;27:325-333.
30. Kienhuis AS, Soeteman-Hernandez LG, Bos PM, Cremers HW, Klerx WN, Talhout R. Potential harmful health effects of inhaling nicotine-free shisha-pen vapor: a chemical risk assessment of the main components propylene glycol and glycerol. *Tob Induc Dis.* 2015;13:1-6.
31. Renne R, Wehner A, Greenspan B, et al. 2-Week and 13-week inhalation studies of aerosolized glycerol in rats. *Inhal Toxicol.* 1992;4:95-111.
32. Herrington JS, Myers C. Electronic cigarette solutions and resultant aerosol profiles. *J Chromatogr A.* 2015;1418:192-199.
33. Eckhardt CM, Baccarelli AA, Wu H. Environmental exposures and extracellular vesicles: indicators of systemic effects and human disease. *Curr Environ Health Rep.* 2022;9:465-476.
34. Pavanello S, Bonzini M, Angelici L, et al. Extracellular vesicle-driven information mediates the long-term effects of particulate matter exposure on coagulation and inflammation pathways. *Toxicol Lett.* 2016;259:143-150.
35. Russell AE, Liao Z, Tkach M, et al. Cigarette smoke-induced extracellular vesicles from dendritic cells alter T-cell activation and HIV replication. *Toxicol Lett.* 2022;360:33-43.
36. Kaur G, Singh K, Maremanda KP, Li D, Chand HS, Rahman I. Differential plasma exosomal long non-coding RNAs expression profiles and their emerging role in E-cigarette users, cigarette, waterpipe, and dual smokers. *PLoS One.* 2020;15:e0243065.
37. Mobarrez F, Antoniewicz L, Hedman L, Bosson JA, Lundbäck M. Electronic cigarettes containing nicotine increase endothelial and platelet derived extracellular vesicles in healthy volunteers. *Atherosclerosis.* 2020;301:93-100.
38. Leventhal AM, Miech R, Barrington-Trimis J, Johnston LD, O'Malley PM, Patrick ME. Flavors of e-cigarettes used by youths in the United States. *JAMA.* 2019;322:2132-2134.
39. Been T, Traboulsi H, Paoli S, et al. Differential impact of JUUL flavors on pulmonary immune modulation and oxidative stress responses in male and female mice. *Arch Toxicol.* 2022;96:1783-1798.
40. Dutta S, Sengupta P. Men and mice: relating their ages. *Life Sci.* 2016;152:244-248.
41. Vucetic A, Filho A, Dong G, Olivier M. Isolation of extracellular vesicles from *Leishmania* spp. *Methods Mol Biol.* 2020;2116:555-574.
42. Carnino JM, Lee H, Jin Y. Isolation and characterization of extracellular vesicles from Broncho-alveolar lavage fluid: a review and comparison of different methods. *Respir Res.* 2019;20:240.
43. Chomczynski P, Mackey K. Short technical reports. Modification of the TRI reagent procedure for isolation of RNA from polysaccharide- and proteoglycan-rich sources. *Biotechniques.* 1995;19:942-945.
44. Ewels P, Magnusson M, Lundin S, Källér M. MultiQC: summarize analysis results for multiple tools and samples in a single report. *Bioinformatics.* 2016;32:3047-3048.
45. Love MI, Huber W, Anders S. Moderated estimation of fold change and dispersion for RNA-seq data with DESeq2. *Genome Biol.* 2014;15:550.
46. Zhou Y, Zhou B, Pache L, et al. Metascape provides a biologist-oriented resource for the analysis of systems-level datasets. *Nat Commun.* 2019;10:1523.
47. Lei W, Zeng DX, Zhu CH, et al. The upregulated expression of OX40/OX40L and their promotion of T cells proliferation in the murine model of asthma. *J Thorac Dis.* 2014;6:979-987.
48. Guo J, Johansson I, Mkrtchian S, Ingelman-Sundberg M. The CYP2W1 enzyme: regulation, properties and activation of prodrugs. *Drug Metab Rev.* 2016;48:369-378.

49. Carnino JM, Lee H. Extracellular vesicles in respiratory disease. *Adv Clin Chem.* 2022;108:105-127.
50. Glynos C, Bibli S-I, Katsaounou P, et al. Comparison of the effects of e-cigarette vapor with cigarette smoke on lung function and inflammation in mice. *Am J Physiol Lung Cell Mol Physiol.* 2018;315:L662-L672.
51. Sussan TE, Gajghate S, Thimmulappa RK, et al. Exposure to electronic cigarettes impairs pulmonary anti-bacterial and antiviral defenses in a mouse model. *PLoS One.* 2015;10:e0116861.
52. Larcombe AN, Janka MA, Mullins BJ, Berry LJ, Bredin A, Franklin PJ. The effects of electronic cigarette aerosol exposure on inflammation and lung function in mice. *Am J Physiol Lung Cell Mol Physiol.* 2017;313:L67-L79.
53. Galli SJ, Borregaard N, Wynn TA. Phenotypic and functional plasticity of cells of innate immunity: macrophages, mast cells and neutrophils. *Nat Immunol.* 2011;12:1035-1044.
54. Domagala-Kulawik J. Effects of cigarette smoke on the lung and systemic immunity. *J Physiol Pharmacol.* 2008;59 Suppl 6:19-34.
55. Holt PG. Immune and inflammatory function in cigarette smokers. *Thorax.* 1987;42:241-249.
56. Taha HR, Al-Sawalha NA, Alzoubi KH, Khabour OF. Effect of E-cigarette aerosol exposure on airway inflammation in a murine model of asthma. *Inhal Toxicol.* 2020;32:503-511.
57. Szafran BN, Pinkston R, Perveen Z, et al. Electronic-cigarette vehicles and flavoring affect lung function and immune responses in a murine model. *Int J Mol Sci.* 2020;21:1-22.
58. Lamb T, Muthumalage T, Meehan-Atrash J, Rahman I. Nose-only exposure to cherry- and tobacco-flavored E-cigarettes induced lung inflammation in mice in a sex-dependent manner. *Toxics.* 2022;10:1-11.
59. Kaplan MJ, Radic M. Neutrophil extracellular traps: double-edged swords of innate immunity. *J Immunol.* 2012;189:2689-2695.
60. Qiu SL, Zhang H, Tang QY, et al. Neutrophil extracellular traps induced by cigarette smoke activate plasmacytoid dendritic cells. *Thorax.* 2017;72:1084-1093.
61. Corriden R, Moshensky A, Bojanowski CM, et al. E-cigarette use increases susceptibility to bacterial infection by impairment of human neutrophil chemotaxis, phagocytosis, and NET formation. *Am J Physiol Cell Physiol.* 2020;318:C205-C214.
62. Eapen MS, Hansbro PM, McAlinden K, et al. Abnormal M1/M2 macrophage phenotype profiles in the small airway wall and lumen in smokers and chronic obstructive pulmonary disease (COPD). *Sci Rep.* 2017;7:13392.
63. Davis ES, Ghosh A, Coakley RD, et al. Chronic E-cigarette exposure alters human alveolar macrophage morphology and gene expression. *Nicotine Tob Res.* 2022;24:395-399.
64. Scott A, Lugg ST, Aldridge K, et al. Pro-inflammatory effects of e-cigarette vapour condensate on human alveolar macrophages. *Thorax.* 2018;73:1161-1169.
65. Park H-R, O'Sullivan M, Vallarino J, et al. Transcriptomic response of primary human airway epithelial cells to flavoring chemicals in electronic cigarettes. *Sci Rep.* 2019;9:1400.
66. Wang L, Wang Y, Chen J, et al. Comparison of biological and transcriptomic effects of conventional cigarette and electronic cigarette smoke exposure at toxicological dose in BEAS-2B cells. *Ecotoxicol Environ Saf.* 2021;222:112472.
67. Tyagi S, Gupta P, Saini AS, Kaushal C, Sharma S. The peroxisome proliferator-activated receptor: a family of nuclear receptors role in various diseases. *J Adv Pharm Technol Res.* 2011;2:236-240.
68. Rigamonti E, Chinetti-Gbaguidi G, Staels B. Regulation of macrophage functions by PPAR-alpha, PPAR-gamma, and LXRs in mice and men. *Arterioscler Thromb Vasc Biol.* 2008;28:1050-1059.
69. Fujii W, Kapellos TS, Baßler K, et al. Alveolar macrophage transcriptomic profiling in COPD shows major lipid metabolism changes. *ERJ Open Res.* 2021;7:1-16.
70. Davies P, Sornberger GC, Huber GL. The stereology of pulmonary alveolar macrophages after prolonged experimental exposure to tobacco smoke. *Lab Invest.* 1977;37:297-306.
71. FDA. *Lung Illnesses Associated with Use of Vaping Products.* Vol 2019. US Food and Drug Administration; 2019.
72. Layden JE, Ghinai I, Pray I, et al. Pulmonary illness related to E-cigarette use in Illinois and Wisconsin—preliminary report. *N Engl J Med.* 2019;382:903-916.
73. Maddock SD, Cirulis MM, Callahan SJ, et al. Pulmonary lipid-laden macrophages and vaping. *N Engl J Med.* 2019;381:1488-1489.
74. Marrocco A, Singh D, Christiani DC, Demokritou P. E-cigarette vaping associated acute lung injury (EVALI): state of science and future research needs. *Crit Rev Toxicol.* 2022;52:188-220.
75. Ganne N, Palraj R, Husted E, Shah I. E-cigarette or vaping product use-associated lung injury (EVALI) masquerading as COVID-19. *BMJ Case Rep.* 2021;141-4.
76. Gao M, Aveyard P, Lindson N, et al. Association between smoking, e-cigarette use and severe COVID-19: a cohort study. *Int J Epidemiol.* 2022;51:1062-1072.
77. Schaunaman N, Crue T, Cervantes D, et al. Electronic cigarette vapor exposure exaggerates the pro-inflammatory response during influenza A viral infection in human distal airway epithelium. *Arch Toxicol.* 2022;96:2319-2328.
78. Gilpin DF, McGown KA, Gallagher K, et al. Electronic cigarette vapour increases virulence and inflammatory potential of respiratory pathogens. *Respir Res.* 2019;20:267.
79. Akkanti BH, Hussain R, Patel MK, et al. Deadly combination of vaping-induced lung injury and influenza: case report. *Diagn Pathol.* 2020;15:83.
80. Majumdar R, Tavakoli Tameh A, Arya SB, Parent CA. Exosomes mediate LTB4 release during neutrophil chemotaxis. *PLoS Biol.* 2021;19:e3001271.
81. Wang Q, Ahmad Khan N, Muthumalage T, et al. Dysregulated repair and inflammatory responses by e-cigarette-derived inhaled nicotine and humectant propylene glycol in a sex-dependent manner in mouse lung. *FASEB Bioadv.* 2019;1:609-623.
82. Lacy P. Mechanisms of degranulation in neutrophils. *Allergy Asthma Clin Immunol.* 2006;2:1-11.
83. Masso-Silva JA, Moshensky A, Shin J, et al. Chronic E-cigarette aerosol inhalation alters the immune state of the lungs and increases ACE2 expression, raising concern for altered response and susceptibility to SARS-CoV-2. *Front Physiol.* 2021;12:649604.
84. Yoshida M, Minagawa S, Araya J, et al. Involvement of cigarette smoke-induced epithelial cell ferroptosis in COPD pathogenesis. *Nat Commun.* 2019;10:3145.
85. Gerth K, Kodidela S, Mahon M, Haque S, Verma N, Kumar S. Circulating extracellular vesicles containing xenobiotic

- metabolizing CYP enzymes and their potential roles in extrahepatic cells via cell-cell interactions. *Int J Mol Sci.* 2019;201-18.
86. Sies H, Berndt C, Jones DP. Oxidative stress. *Annu Rev Biochem.* 2017;86:715-748.
87. Ooi BG, Dutta D, Kazipeta K, Chong NS. Influence of the E-cigarette emission profile by the ratio of glycerol to propylene glycol in E-liquid composition. *ACS Omega.* 2019;4:13338-13348.
88. Sutherland KM, Edwards PC, Combs TJ, Van Winkle LS. Sex differences in the development of airway epithelial tolerance to naphthalene. *Am J Physiol Lung Cell Mol Physiol.* 2012;302:L68-L81.
89. Rock JR, Randell SH, Hogan BL. Airway basal stem cells: a perspective on their roles in epithelial homeostasis and remodeling. *Dis Model Mech.* 2010;3:545-556.
90. Tyler WS. Comparative subgross anatomy of lungs. Pleuras, interlobular septa, and distal airways. *Am Rev Respir Dis.* 1983;128:S32-S36.
91. Phillips CG, Kaye SR. On the asymmetry of bifurcations in the bronchial tree. *Respir Physiol.* 1997;107:85-98.

SUPPORTING INFORMATION

Additional supporting information can be found online in the Supporting Information section at the end of this article.

How to cite this article: Been T, Alakhtar B, Traboulsi H, et al. Chronic low-level JUUL aerosol exposure causes pulmonary immunologic, transcriptomic, and proteomic changes. *The FASEB Journal.* 2023;37:e22732. doi:[10.1096/fj.202201392R](https://doi.org/10.1096/fj.202201392R)